This paper has been accepted for publication in Composites Part A: Applied Science and Manufacturing

The effect of transverse compressive stresses on tensile failure of carbon fibre/epoxy composites

Tamas Rev[1,2*], Michael R. Wisnom[2], Xiaodong, Xu[2,3], Gergely Czél[4]

[1]Technion - Israel Institute of Technology, Materials Mechanics Centre, Technion City, 32000, Haifa, Israel

[2]Bristol Composites Institute, University of Bristol, Queen's Building, Bristol BS8 1TR, United Kingdom

[3]University of the West of England, Frenchay Campus, Coldharbour Lane, Bristol BS16 1QY, United Kingdom

[4]Department of Polymer Engineering, Faculty of Mechanical Engineering, Budapest University of Technology and Economics, Műegyetem rkp. 3., H-1111 Budapest, Hungary

*corresponding author, e-mail: tamas.rev@campus.technion.ac.il

Abstract

A novel test configuration has been developed to induce combined stress-states of in-plane longitudinal tension and transverse compression in thin-ply, unidirectional (UD) composite layers. Three different multi-directional laminates have been designed incorporating UD carbon/epoxy plies embedded in angle-ply blocks of the same material. The scissoring deformation of the angle-ply blocks induces transverse compression in the central UD layers when the composite is strained in the 0° fibre direction. The amount of transverse compressive stress was estimated from the measured surface strain of the laminates to be up to about 140 MPa. Negligible effect was found on the tensile failure strain despite the very high in-plane transverse compressive strains generated in the laminates. These were much higher than those typically attained in multi-directional laminates, exceeding the strain at which

compressive failure would occur in any 90° plies. The results of this study suggest that in practice fibre direction tensile failure is unlikely to be significantly affected by transverse compressive stresses.

Keywords:

Laminates; Strength; Multi-axial loading; Thin-ply;

1. Introduction

The strength prediction of composite materials is hindered by various factors ranging from multiple different failure mechanisms and their interactions with each other to the challenges in defining failure as well as obtaining good experimental data and theories that can reliably support the empirical measurements [1]. As the demand of key industries - such as aerospace and civil engineering - with the largest consumption of composite materials [2,3] is ever- increasing, it is crucial to determine the real behaviour of fibre reinforced polymers (FRP) especially under multi-axial loading resembling realistic operation conditions.

Many failure criteria have been proposed and utilized to tackle the complex issue of predicting the failure of composite materials. Up to now, the most commonly used criteria include the simple stress and strain theories [4,5] as well as the interactive Tsai-Hill [6] and Tsai-Wu [7] criteria. The world's most extensive research program on failure namely 'The World-Wide Failure Exercise' (WWFE) [8–11] in 2013 concluded that there is currently no existing failure criterion that can be universally accepted to predict failure in such fibrous materials. With regard to multi-axial and combined loading, it is hard to validate predictions due to the lack of reliable experimental data [12,13]. A review of multiaxial and biaxial loading tests for composite materials by Chen and Matthews [14] highlighted the issues in biaxial testing mainly on tubular specimens, cruciform specimens and flat plate bending. Thom [15]

also compiled a comprehensive review on biaxial test methods highlighting their characteristic problems. In a more recent study, Olsson [16] presented a survey on test methods to determine the strength of composite laminates with regard to both in-plane and out-of-plane loadings. The review covered the most commonly used methods for generating multi-axial in-plane loads including tubular specimens [17,18], cruciform specimens [19,20], methods incorporating off-axis [21,22], angle-ply laminates [23,24] and biaxial Arcan tests [25].

Even for unidirectional (UD) laminates, accurately determining their fundamental mechanical properties such as failure strain or failure stress is still a scientific challenge [12]. The ultimate strength of UD carbon/epoxy laminates is often underestimated due to the experimental strength measurements being affected by stress concentrations at the end-tab regions of the coupons [26]. Usually, a significant knock-down in their measured strength can be observed accompanied by premature failure of the specimens and notably lower strains. For more complex cases such as testing under biaxial loading conditions, the difficulty in acquiring acceptable data is magnified due to issues that include edge effects, gripping related problems, quality of the materials and the consistency of coupon fabrication and testing [12].

A debatable part of the failure envelope for carbon composites is the tension – compression quadrant, considering the effect of transverse compressive stresses on the longitudinal (fibre) direction tensile strength. A two-dimensional, strain based maximum shear stress failure criterion for laminates was proposed by Hart-Smith [27] who truncated the failure envelope by a 45° cut off between longitudinal tensile strain and transverse compressive strain. A study carried out by Wisnom [28] investigated the effect of transverse compressive stresses on the tensile failure of glass/epoxy through four point bending tests on angle ply laminates with 0° plies on the surface. It was shown that the fibre direction tensile strength was relatively insensitive to transverse compression. It should be noted that in the study by Wisnom there was a strain gradient due to the nature of bending tests which may have influenced the results.

Additionally, a controversy was also pointed out between Hart-Smith's proposed criterion and some of the supporting experimental results available in the literature. For instance Swanson et al. [29,30] demonstrated empirical evidence that supports the conclusion of fibre tensile failure not being sensitive to transverse normal and shear stresses. They carried out multiaxial characterisation of different T800/3900-2 carbon composite laminates under combinations of internal pressure, axial tension or compression and torsion. It was concluded that the maximum fibre direction strain criterion is a simple and accurate option to utilize when assessing ultimate failure. Sun and Quinn [31] carried out in-plane tests on off-axis laminates that contained adhesive films between the plies. The maximum stress and strain criteria reportedly gave a better fit than Tsai-Hill, even though the former was slightly unconservative, as also concluded in [28].

To resolve this question, this study aims to find out the true effect of transverse compressive stresses on the fibre failure strain of unidirectional (UD) carbon/epoxy composites. A novel approach based on thin-ply laminates of unidirectional (UD) and angle-plies is presented which overcomes the key problems of previous tests. The bi-axial stress state in the 0° plies is indirectly applied in a tensile test set-up where the contraction of the angle-plies induces compression in the central UD layer when the composite is strained in the longitudinal direction. Compliant surface angle-ply blocks are used to eliminate stress concentrations at the tabs, and dispersed thin plies to avoid transverse cracking and edge delamination. The test method proposed here offers a reliable solution for acquiring accurate experimental data on this particular biaxial loading scenario and has the benefits of repeatability and ease of use.

2. Concept

The main objective of this study is to investigate the interaction between in-plane transverse compression and longitudinal tension in carbon epoxy laminates through a thin-ply tensile test-based method. There are numerous variables addressed throughout design including (i) the issue of avoiding stress concentrations, (ii) the need for utilizing thin-plies to avoid free-edge delamination as well as (iii) the issue of avoiding potential hybrid effects. Discussion of these is given in the following paragraphs. A schematic of a typical specimen configuration and the proposed concept is illustrated in Figure 1.

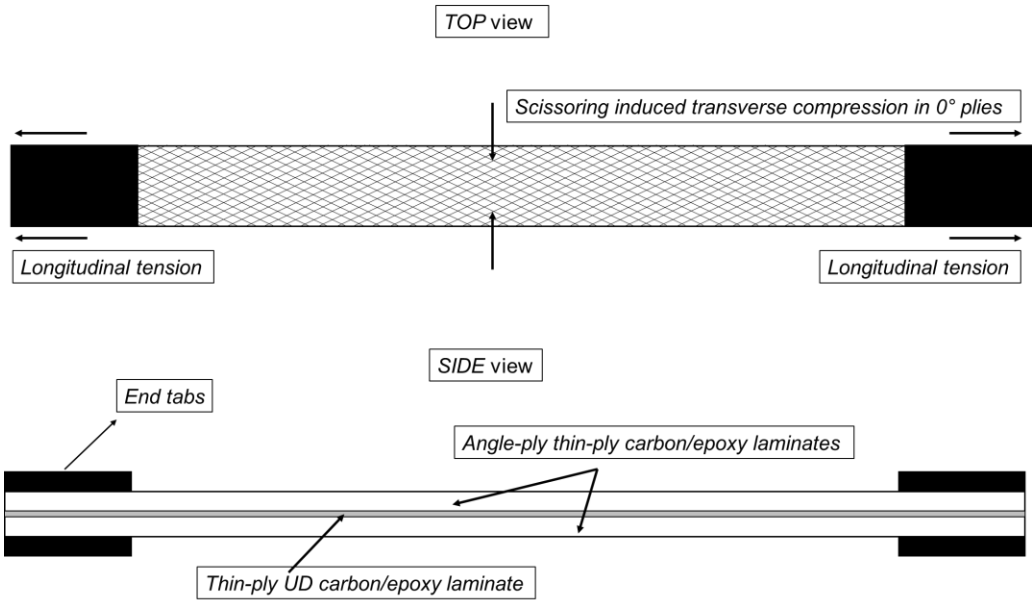

Figure 1. Top and side view schematic of the thin-ply UD laminate embedded in thin-ply, angle-ply blocks (for larger angles)

Czél et al [26] proposed an interlayer hybrid specimen type consisting of UD carbon/epoxy in between protective glass/epoxy layers for eliminating the stress concentrations near the end-tabs during tensile testing. Consistent gauge section failure of the UD carbon layers was reported when determining the tensile failure strains. Further benefit is that there was no need for optimising the gripping conditions as the stress concentrations at

the grips were eliminated. The glass layers in this case also protected the carbon plies from the rough grip faces, so no additional end-tabs were necessary. In this study, the thin-ply angle-ply carbon/epoxy blocks can play the role of the glass/epoxy protective layers in eliminating the stress concentrations, since they can withstand high strains due to scissoring. On the other hand, the measured values were significantly higher than those obtained from conventional non-hybrid carbon/epoxy specimens. It was previously shown by Wisnom *et al.* [33] that thin UD plies surrounded by higher elongation layers show an increase in their failure strain due to the constraint on forming a critical cluster of fibre breaks, commonly referred to as the hybrid effect. With regard to the test procedure and specimen design, this hybrid effect is unwanted and therefore we aimed at avoiding it by design. Wisnom *et al.* [33] presented that single (0.03 mm) and double thin plies (0.06 mm) of TR30 carbon/epoxy placed between S-glass/epoxy exhibited significantly higher failure strains than those of the configurations with three (0.09 mm) and four layers (0.12 mm). This means that the observed hybrid effect fades away above a carbon/epoxy layer thickness limit (which was around 0.09 mm for the tested material). Based on the previous study, four thin plies of similar thin carbon/epoxy were utilized in the investigated hybrid laminates to avoid the hybrid effect.

Thin-ply composite materials were utilised mainly to ensure that the designed laminates will fail in the desired manner, and damage mechanisms such as free-edge delamination (a predominant failure mechanism for angle-ply laminates) and (transverse) matrix cracking do not precede nor influence the desired overall longitudinal fibre failure mode in the central UD plies. Thin-ply materials have previously shown to be able to delay and suppress the above mentioned damage mechanisms (transverse microcracking [34] and free-edge delamination [35,36]) in different loadings - static, fatigue and impact as reviewed by Cugnoni *et al.* [37]. Extensive reviews of thin-ply polymer composites including their manufacture, microstructure, mechanical performance, and the implications for structural design and application prospects

were presented by Galos [38] and Arteiro *et al.* [39]. It was also reported that the advantages of using thin-plies, achieving a higher onset of damage such as microcracking or delamination in the composites, come with a change in the failure mode of the laminates: shifting from a more complex, multi-mode failure with significant delamination to a quasi-brittle failure governed by fibre fracture in the 0° plies. These materials represent a new generation of advanced composites that provide a promising approach to exploit the true potential for carbon fibre composite structures especially by delaying the onset of damage up until a fibre dominated failure is achieved.

3. Experimental

3.1. Materials

The materials considered in this study were a thin-ply TC33 carbon fibre produced by Formosa Plastics and a standard ply thickness S-Glass material supplied by Owens Corning. The incorporating resin systems for both materials were 125 °C cure epoxies. The matrix for the carbon was a K51 resin system supplied by Skyflex and for the glass fibre a 913 resin system supplied by Hexcel. The resin systems were compatible with each other.

Basic properties of the applied fibre and prepreg systems are presented in Table 1 and Table 2 respectively.

Table 1. Fibre properties of the applied unidirectional prepregs based on manufacturers data

Fibre type	Elastic modulus [GPa]	Density [g/cm^3]	Strain to failure [%]	Tensile strength [GPa]
Tairyfil TC33 carbon	230	1.8	1.5	3.45
FliteStrand S ZT S-Glass [26]	88	2.45	5.5	4.8 – 5.1

Table 2. Cured ply properties of the applied unidirectional prepregs

Prepreg type	Areal density [g/m^2]	Cured ply thickness [μm]	Fibre volume fraction [%]	Initial elastic modulus [GPa]	Tensile strain to failure [%]	CTE α_L [1/K]	CTE α_T [1/K]
TC33/K51 carbon/epoxy	21[a]	30[a]	39[a]	95.3[a]	1.61[a]	$-1 \cdot 10^{-6}$ [c]	$4 \cdot 10^{-5}$ [c]
S-Glass/913 glass/ epoxy	190[b]	155[b]	51[b]	45.7[b]	3.98[b]	$2 \cdot 10^{-6}$ [c]	$3 \cdot 10^{-5}$ [c]

[a]Based on measurements
[b]Based on [26]
[c]Estimated based on reported values for T300/5208 in [40] for the carbon and [26] for the glass

3.2. Configuration design

To be able to determine the interaction between transverse compression and longitudinal tension in the most accurate way possible, it is important to minimise other stress components present in the UD laminate.

To eliminate shear, the multi-axial stress state is indirectly applied to the UD layers: the central thin-ply UD carbon/epoxy layer is embedded in thin-ply angle-ply blocks of carbon/epoxy, where the scissoring deformation of the angle plies induces the transverse compressive loading on the central UD layers as shown in Figure 1.

Furthermore, the laminate as a whole is designed to be balanced and symmetric. This way the in-plane shear coupling terms (A_{16}, A_{26}) and the extension- bending coupling (B matrix) are zero in the ABD matrices of the laminates.

The configurations were also designed in order to induce various levels of transverse compression in the central UD layers: by varying the angle of the embedding plies, different amounts of transverse stress are generated when the composite specimens are strained in the longitudinal direction. The key influencing parameters for the amount of transverse compression generated are the angle and the relative thickness of the angle-ply blocks. The transverse compression arises from the Poisson's ratio mismatch between the angle-ply blocks

and the UD laminate. By maximizing this mismatch and choosing an optimum angle, the transverse compression can be maximized in the central UD layers. Furthermore, increasing the number of angle-ply pairs in the blocks increases the magnitude of the transverse stresses put on the central UD layers.

The selection of the stacking sequences was carried out in MATLAB software using Classical Laminate Theory (CLT) assuming a plane stress state for the composite laminates [41]. An illustration of varying amounts of transverse to longitudinal stress ratios arising in the central UD layers as a function of the angle of the angle-ply blocks is shown in Figure 2. The applied strain for the generated curves was 1.61 % (measured failure strain of the carbon in Table 2) and the analysis was initially carried out using estimated linear material properties as shown in Table 2.

The absolute thickness of the central UD layers plays an important role in ensuring that any hybrid effects are avoided. A minimum thickness for the carbon of 0.12 mm was therefore chosen, equivalent to four plies of the utilized thin-ply high-strength carbon/epoxy material.

Alternatively, one single thicker ply could be utilized in this concept, although thin angle plies would still be needed to avoid premature damage there.

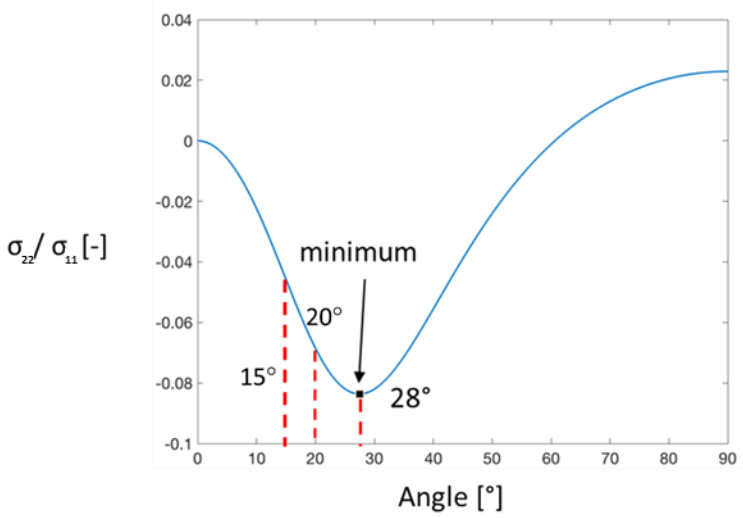

Figure 2. Transverse compressive stress to longitudinal stress ratios as a function of the angle of the embedding angle-ply blocks: the chosen angles are marked with red dashed lines on the curve. The exact lay-up sequences for the chosen angles were $[\pm 15_6/0_2]_s$, $[\pm 20_6/0_2]_s$, and $[\pm 28_6/0_2]_s$ respectively.

Overall, four different configurations were designed including the specimens that were used to determine the accurate baseline failure strain of the utilised carbon fibre/epoxy material. A summary of all the configurations is shown in Table 3, where SG denotes the S-Glass layers in the laminates.

Table 3. Specimen configurations

Configuration	No. of specimens tested [-]	Measured overall thickness [mm]
$[SG_2/0_2]_s$-UD hybrid baseline	8	0.768
$[SG_2/\pm 15_6/0_2]_s$	7	1.494
$[\pm 20_6/0_2]_s$	7	0.798
$[\pm 28_6/0_2]_s$	6	0.806

All coupons tested in the experimental campaign were parallel edge tensile specimens as illustrated in Figure 1 with the nominal dimensions of 270/190/20 mm overall length/gauge length/width respectively.

For the configuration with the shallower angle (15°) embedding the central UD block, the surface plies do not provide sufficient 'protection' against stress concentrations at the grips due to their relatively high stiffness. Hence, the design presented in Figure 1 has incorporated additional layers of glass/epoxy in a similar manner to that described in [26] but without the inclusion of end-tabs. This way, it was ensured that stress concentrations at the grips were eliminated so that consistent gauge section failures were expected. The baseline configuration was similarly constructed, based on [26].

For the specimens with increased angle of the angle-ply blocks (20°and 28° configuration), the additional glass layers were omitted and carbon only specimens were fabricated with end-tabs as shown in Figure 1.

3.3. Specimen fabrication

All laminates were manufactured by a conventional prepreg curing process. After hand-lay-up of the specific plies, a vacuum bag was utilised on a flat aluminium tool plate. There were additional silicone sheets placed on top of the laminates in order to ensure a smooth top surface and an even distribution of the autoclave pressure on the laminates.

The composite plates with only carbon layers were cured at the recommended temperature and pressure cycles provided by the manufacturer: 30 mins at 80°C and 90 mins at 125°C with 0.7 MPa applied pressure and a heating rate of 2°C/min. For the hybrid configurations (carbon/glass), - since both resin systems were similar -, only the ramp-up, cool down rate and any dwells occurring was adjusted by using the longer of the recommended

cycles from the different prepreg manufacturers: 60 mins at 80°C and 100 mins at 125°C with 0.7 MPa applied pressure and a heating rate of 2°C/min.

After curing, the composite plates were cut into the desired geometry by a Computer Numerical Controlled (CNC) diamond wheel. Untapered, 1.7 mm thick composites made of glass fibre fabric/epoxy was used as end-tabs for two of the configurations. The end-tabs were bonded to the specimens using an Araldite 2014/1 epoxy adhesive system. The samples with end tabs were then put into an atmospheric oven to cure the adhesive for 120 min at 80°C.

3.4. Testing method

Mechanical testing of the specimens was carried out on an Instron 8801, computer controlled, universal servo-hydraulic test machine equipped with Instron 2743-401 type hydraulic wedge grips and a 100 kN load cell. The grips had 50 mm wide Instron 2704-521 type serrated steel jaw faces. The uniaxial tensile loading was introduced under displacement control at a crosshead speed of 2 mm/min as per the ASTM D3039 standard. Clamping pressure was kept as low as possible to minimise end tab failures yet avoiding any slippage at the grips. Longitudinal and transverse strains were measured over the maximum possible gauge lengths of 180 mm and 15 mm respectively using an Imetrum video extensometer system, with the test machine outputting the corresponding force signals. The high-definition extensometer videos recorded during the tests were kept for further analysis.

4. Results and discussion

4.1. Baseline configuration

When the hybrid baseline specimens were loaded, the fracture of the carbon layer resulted in delamination between the carbon and the embedding glass layers along the gauge

length of the specimens. A typical response of such hybrid specimens is presented in Figure 3 reproduced from [26]. Since the objective was to extract the failure strain of the UD material, the coupons were not loaded extensively beyond the first significant load drop that corresponds to the 0° carbon layer failure (point 1 on Figure 3). However, if loaded further after the first load drop (point 2 on Figure 3), residual load bearing behaviour due to the high elongation glass layers would be observed.

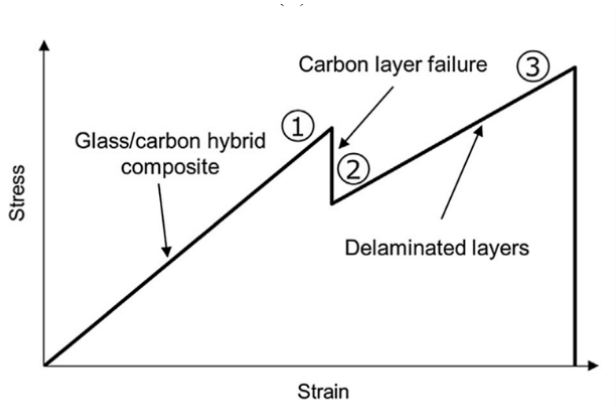

Figure 3. Stress-strain response of UD glass/carbon hybrid specimens reproduced from [26]

Figure 4 (a) shows the stress strain curves of the tested hybrid glass/carbon baseline configuration up to the first load drop. The fracture of the carbon layer in the centre of the light (orange) coloured delaminated area can be seen in Figure 4 (b).

It should be noted that the results are affected by small residual thermal strains that originate from the mismatch in the Coefficient of Thermal Expansion (CTE) of the different plies. Residual thermal strains were calculated from force-equilibrium between the carbon/epoxy and glass/epoxy layers assuming constant strain through the thickness and a 100°C temperature drop from the cure temperature to room temperature. The CTE values used for the different prepregs can be found in Table 2. For the longitudinal direction, the properties of a similar grade carbon fibre with the same matrix [40], and the same glass/epoxy

[26] were utilised and for the transverse direction, estimates from the literature for similar materials were utilized.

The results of the baseline tests including the correction with the calculated residual thermal strains are summarised in Table 4. This table also includes the test results of a non-hybrid baseline: 16 layers of the same TC33/K51 carbon/epoxy material. The moderate increase (10%) in the failure strain of the hybrid specimens can be attributed to the elimination of stress concentrations and the associated premature failure.

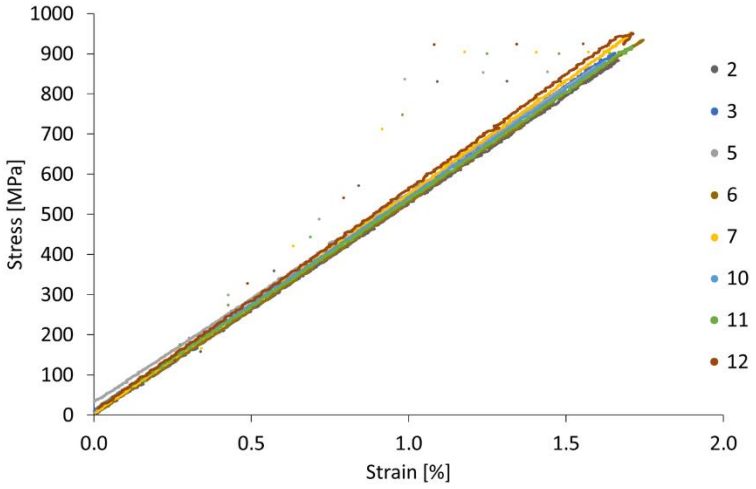

(a)

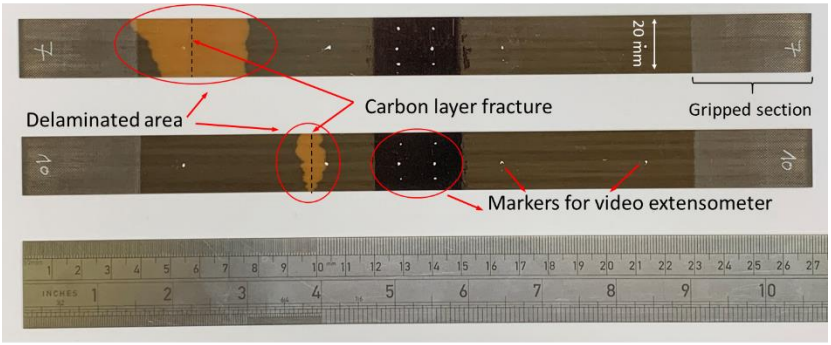

(b)

Figure 4. (a) Mechanical test results of the hybrid glass/carbon baseline configuration with (b) illustration of the behaviour of typical tested coupons: the carbon layer fracture was followed by sudden delamination from the embedding glass layers. The specimens did not incorporate end-tabs and all had gauge section failures

Table 4. Baseline tensile test results for the TC33/K51 material in a non-hybrid and hybrid configuration and thermal residual strain correction

Configuration	No. of specimens tested [-]	Measured carbon layer failure strain [%] (C.o.V.[%])	Corrected carbon layer failure strain [%]
$[0_{16}]$- non-hybrid UD baseline	9	1.50 (4.8%)	-
$[SG_2/0_2]_s$ - hybrid UD baseline	8	1.65 (3.0%)	1.62

4.2. Angle-ply/UD configurations

Figure 5 (a) – (f) illustrates the typical stress-strain responses of the different angle-ply/UD laminates. All stresses presented are remote stresses. It can be seen in Figure 5 (a) – (b) that for the shallower angled $[SG_2/\pm15_6/0_2]_s$ configuration, both the longitudinal and transverse strain responses are approximately linear up to failure. The observed small stiffening in the 15° case is most probably due to the intrinsic non-linearity of the central UD carbon/epoxy block. In the larger angle cases the softening due to scissoring and matrix plasticity of the angle-ply blocks are more significant. For the larger angle configurations - $[\pm20_6/0_2]_s$ and $[\pm28_6/0_2]_s$ respectively – a small, gradual stiffness degradation in the response of the laminates can be observed. The responses become more non-linear, especially in the transverse direction. The non-linearity observed is mainly associated with the angle-ply blocks surrounding the unidirectional material: there is no in-plane shear arising at the laminate level, however there is substantial in-plane shear expected at the lamina level in the angle-ply blocks. Besides, the indirectly applied transverse compression also plays a role in the non-linear character of the transverse strain curves.

In the experimental campaign, primarily surface strains are considered because they can be directly acquired by the video extensometer. Both longitudinal and transverse strains are directly measured on the surface of the specimens. Since it can be assumed that they are constant through the thickness of the laminate, they can be used as the strains in the central UD layers. A summary of the measured strains (ε_{xx}, ε_{yy}) and the macroscopic laminate stresses at failure (σ_{xx}) including the baseline measurements are shown in Table 5. All values are averages for each set of the tested specimens with the variability included in the table and they represent the strain at failure corresponding to the first significant load drop of the specimens.

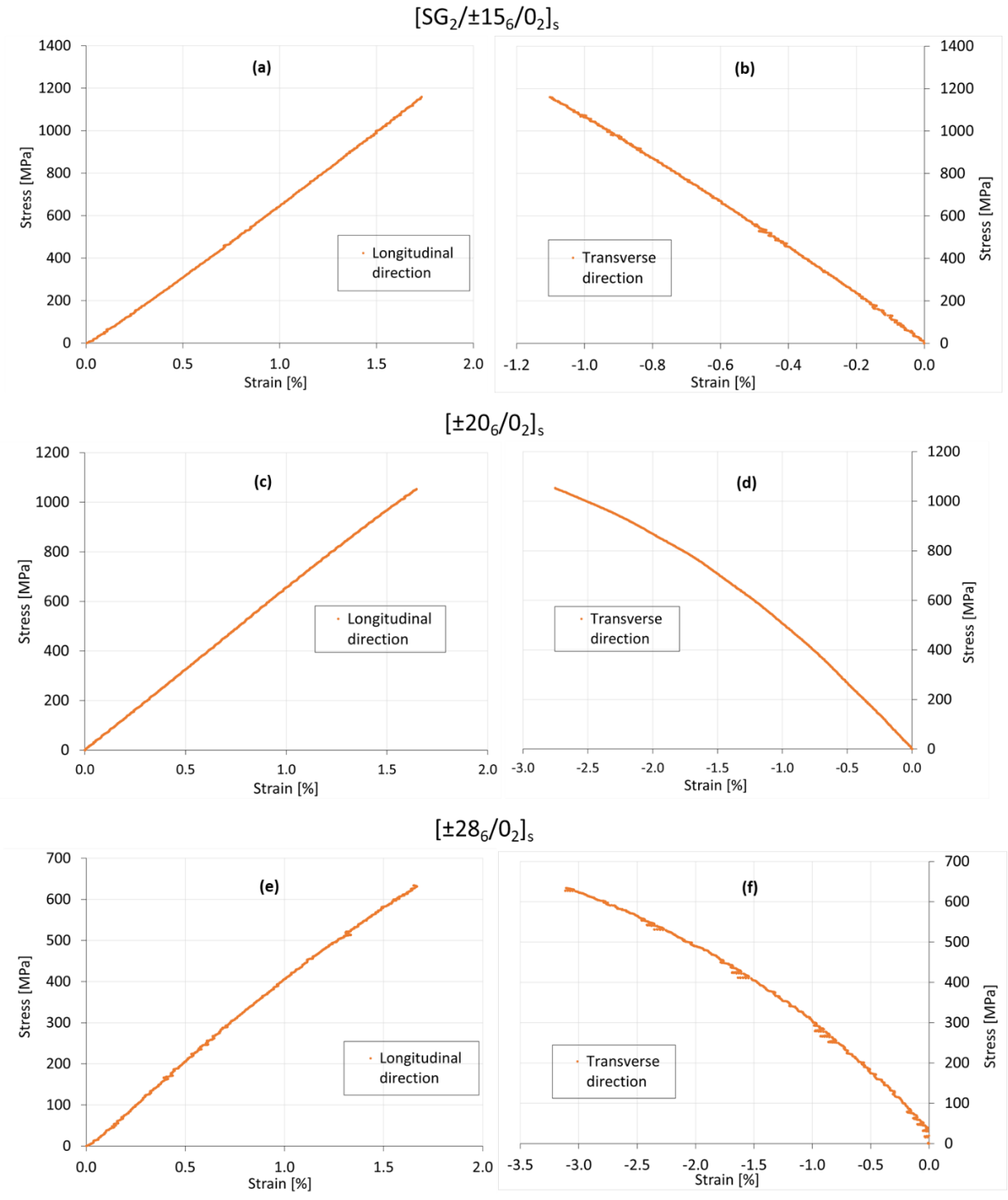

Figure 5. Typical stress – strain responses of the different angle-ply/UD configurations: (a) – (b) - $[SG_2/\pm15_6/0_2]_s$, (c) – (d) - $[\pm20_6/0_2]_s$, and (e) – (f) - $[\pm28_6/0_2]_s$ respectively. The graphs represent the different measured strains in both longitudinal and transverse directions. All stresses presented are remote stresses.

Table 5. Summary table of the measured strains and the average applied remote stresses at the fracture of the UD carbon/epoxy

Configuration	ε_{xx} [%] (C.o.V. [%])	ε_{yy} [%] (C.o.V. [%])	σ_{xx} [MPa] (C.o.V. [%])
Baseline $[SG_2/0_2]_s$	1.65 (3.0)	-0.50 (5.0)	900 (3.7)
$[SG_2/\pm15_6/0_2]_s$	1.60 (5.1)	-1.04 (6.4)	1092 (4.4)
$[\pm20_6/0_2]_s$	1.62 (3.2)	-2.84 (7.7)	1053 (3.5)
$[\pm28_6/0_2]_s$	1.62 (1.9)	-2.91 (4.5)	625 (2.7)

As can be seen, there were very high in-plane transverse compressive strains in the central UD block of the larger angle angle-ply configurations: 2.84 % and 2.91 % for the 20° and 28° angles respectively with a transverse to longitudinal strain ratio of 1.46 and 1.49. The transverse strains are more similar than expected from the initial calculations shown in Fig. 2 due to the effect of material non-linearity. The measured data is illustrated in Figure 6 showing the overall longitudinal failure strains as a function of the overall transverse strains for the different configurations including the baseline tests. The thermal residual strains have only a small effect on the overall measured strains hence they are not included in Figure 6 below, but they are accounted for in terms of stresses calculated in Section 4.2.2.

When compared with the measured baseline failure strain (1.65%), the trend suggests that high in-plane transverse compressive strains do not significantly influence the longitudinal failure strain of the UD carbon/epoxy material. For instance, in a typical quasi-isotropic (QI) laminate, the 90° ply would fail in fibre compression before the laminate reaches -1.5 % transverse compressive strain.

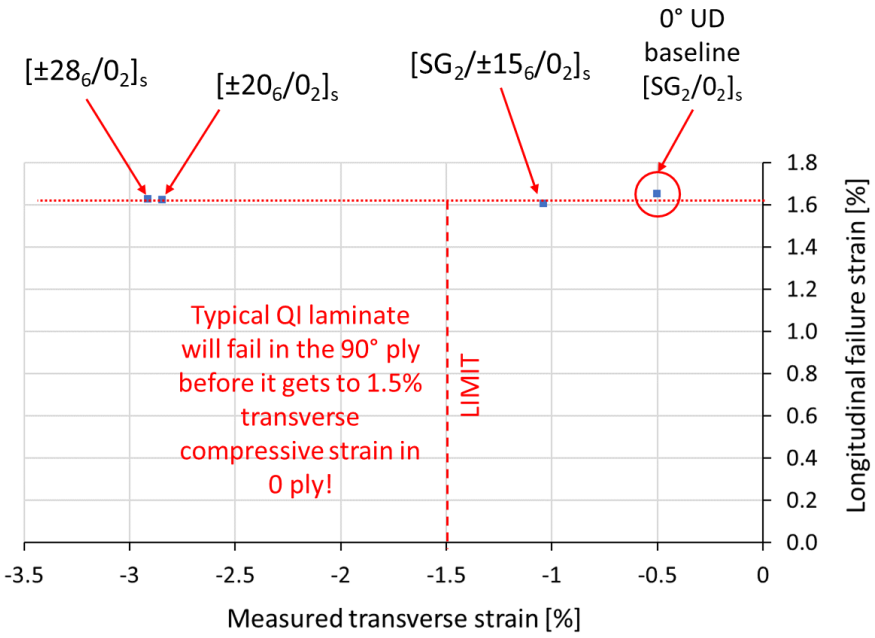

Figure 6. The longitudinal strain to failure of the UD carbon/epoxy as a function of the overall measured transverse strains for all configurations including the baseline tests (not corrected for thermal residual strains)

4.2.1. Determination of transverse stresses

Since transverse stresses cannot be measured directly, they have to be calculated from the measured strains. The fibres in the central 0° UD block experience transverse strain that is not only due to the effect of the surrounding angle-plies but also from the Poisson's contraction of the UD material. In other words, even if the central UD block did not experience any compression from the neighbouring ply blocks, it would still have transverse strain in the material.

Consequently, to determine the transverse compressive stresses, the measured strains are converted into stresses using the orthotropic stress-strain equations with linear assumptions as shown in Equation 1 and 2. The utilized material properties for the TC33/K51 carbon/epoxy lamina are based on empirical measurements and can be found in Table 6.

Table 6. Measured basic material properties of the TC33/K51 lamina

	E_{11} [GPa]	E_{22} [GPa]	ν_{12} [-]	ν_{21}* [-]	G_{12} [GPa]
TC33/K51 carbon/epoxy	95.3	6.1	0.301	0.019	2.47

*Calculated from ν_{12}

$$\sigma_{11}^{0} = \frac{E_{11}}{1-\nu_{12}\nu_{21}}\varepsilon_{xx} + \frac{\nu_{12}E_{22}}{1-\nu_{12}\nu_{21}}\varepsilon_{yy} \quad (1)$$

$$\sigma_{22}^{0} = \frac{\nu_{12}E_{22}}{1-\nu_{12}\nu_{21}}\varepsilon_{xx} + \frac{E_{22}}{1-\nu_{12}\nu_{21}}\varepsilon_{yy} \quad (2)$$

where E_{11} and E_{22} represent the longitudinal and transverse direction moduli, ε_{xx} and ε_{yy} the measured longitudinal and transverse surface strain and ν_{12} and ν_{21} the major and minor Poisson's ratios respectively. Equation (2) represents the mechanical transverse compressive stresses generated in the central UD layers (σ_{22}^{0}).

A summary of the measured strains and the calculated mechanical stresses using linear assumptions (σ_{11}^{0} and σ_{22}^{0}) are presented in Table 7. The ratios of transverse to fibre direction stresses are slightly different from those shown in Fig. 2 because the latter were based on estimated material properties.

Table 7. Summary table of the measured strains and the calculated mechanical stresses using linear assumptions

Configuration	ε_{xx} [%] (C.o.V. [%])	ε_{yy} [%] (C.o.V. [%])	σ_{11}^{0} [MPa]	σ_{22}^{0} [MPa]
Baseline $[SG_2/0_2]_s$	1.65 (3.0)	-0.50 (5.0)	1572	-0.5
$[SG_2/\pm15_6/0_2]_s$	1.60 (5.1)	-1.04 (6.5)	1516	-33
$[\pm20_6/0_2]_s$	1.62 (3.2)	-2.84 (7.7)	1502	-145
$[\pm28_6/0_2]_s$	1.62 (1.9)	-2.91 (4.5)	1504	-149

4.2.2. Thermal residual stresses

The calculated stresses of the central UD block need to be corrected for thermal residual stresses arising in the laminate as a result of the mismatch in CTE between the angle-ply and UD blocks. These calculations are based on CLT assuming linear elastic response. The corrections are presented in Table 8.

The elastic strain $[\varepsilon_{el,c}]$ of the multi-directional laminate is associated with the residual stresses that are caused by the constraint from other plies. In the case of the central UD carbon layers it is determined as the difference between the total strain of the laminate $[\varepsilon^{total}]$ and the free thermal strain of the central carbon layers $[\varepsilon_{t,c}]$ as follows:

$$[\varepsilon_{el,c}] = [\varepsilon^{total}] - [\varepsilon_{t,c}] \qquad (3)$$

Once the elastic strains of the central block are determined, the residual stresses can be calculated using Classical Laminate Theory (CLT) in the following way:

$$[\sigma_{res}] = [Q^*][\varepsilon_{el,c}] \qquad (4)$$

where Q^* represents the reduced stiffness matrix of the UD carbon block.

The calculated residual thermal stresses for the central UD carbon block (σ_{res}) and the estimated longitudinal $(\sigma_{11}^{0^*})$ and transverse stresses $(\sigma_{22}^{0^*})$ including thermal corrections for each configuration can be found in Table 8. The free thermal strains were estimated to be 0.010 % for the longitudinal direction and -0.40 % for the transverse direction in the central UD carbon layers respectively based on the CTE values given in Table 2.

All the corrected stresses presented are based on the measured strain to failure values found in Table 5. The arising thermal residual stresses presented are not significant in magnitude.

Table 8. Summary of the thermal residual stress corrections in the central UD layers

Configuration	Longitudinal σ_{res} [MPa]	Transverse σ_{res} [MPa]	σ_{11}^{0} [MPa] (C.o.V. [%])	Corrected $\sigma_{11}^{0^*}$ [MPa]	σ_{22}^{0} [MPa] (C.o.V. [%])	Corrected $\sigma_{22}^{0^*}$ [MPa]
Baseline $[SG_2/0_2]_s$	-19.0	5	1572 (0.0)	1553	-0.5 (3.2)	4.5
$[SG_2/\pm15_6/0_2]_s$	4.6	4.2	1516 (5.6)	1521	-33 (7.3)	-29.3
$[\pm20_6/0_2]_s$	32.2	3.5	1502 (3.2)	1534	-145 (9.2)	-141.1
$[\pm28_6/0_2]_s$	48.9	8.3	1504 (1.8)	1553	-149 (5.2)	-140.4

4.2.3. Summary

Figure 7 illustrates the estimated fibre direction failure stresses as a function of the estimated transverse stresses at failure in the central UD block, taking account of the Poisson contraction and thermal residual stresses in the laminates.

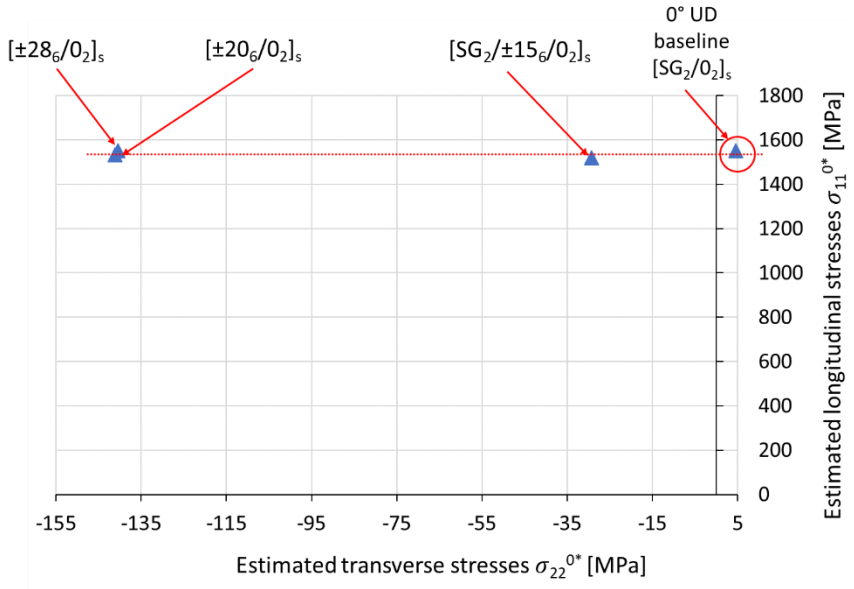

Figure 7. The estimated transverse stresses as a function of the longitudinal stresses at failure in the central UD carbon block, including corrections for the Poisson contraction and the thermal residual stresses

This linear approach to estimate the transverse stresses in the central UD block is a simple method based on the directly measured strains. It shows a very similar trend to what is found in Figure 6: transverse stress does not affect the fibre failure stress significantly.

However, when investigating the transverse compressive response of the utilized TC33/K51 material, a highly non-linear behaviour can be observed as shown in Figure 8.

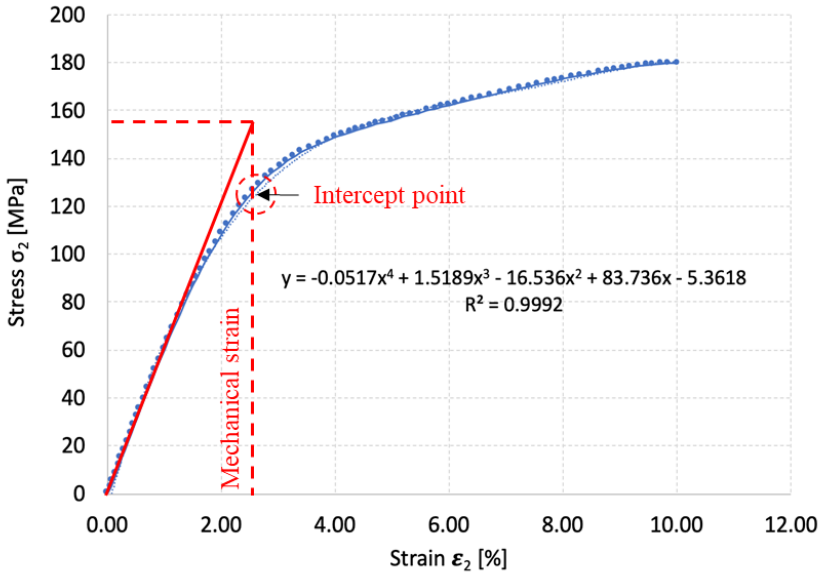

Figure 8. Transverse compressive stress-strain curve adapted from [42]

The material response was taken from the characterisation tests of Fuller [42] which were acquired on a similar material using the same resin system (K51 by Skyflex) and a similar fibre from a different manufacturer (TR30 by Mitsubishi Rayon). The TR30/K51 prepreg exhibited a similarly low fibre volume fraction of 42.5% compared to 39.1% for the TC33/K51, and the initial transverse modulus of the material was 6 GPa, very similar to the 6.1 GPa measured for the thin-ply prepreg utilized in this study.

The measured transverse strains ε_{yy} (see Table 7) do not go far beyond the initial linear region of the material response in Figure 8 (which is to the left of the red vertical dashed line), and significant non-linear behaviour is only demonstrated at much higher strains. When

correcting for the Poisson ratio contractions, the mechanical strains responsible for stresses in the 20° and 28° cases are 2.36% and 2.42% respectively with an average value of 2.39% as marked on Figure 8 (with the vertical red dashed line). The corresponding stress estimated at this average strain is a maximum transverse stress of 155 MPa (red horizontal dashed line) ignoring the effect of the fibre direction stress. This is about 20% higher than the value from the intercept point on the non-linear curve in Figure 8, and so should not greatly affect the previously presented results. The conclusion can be drawn that in-plane transverse compression does not affect the fibre failure strain even if the non-linear behaviour is considered.

4.2.4. Failure analysis

Typical failed specimens of each configuration and their respective failure mechanisms are illustrated in Figure 9. The coupons with the shallower angle lay-up $[SG_2/\pm 15_6/0_2]_s$ failed in the gauge section with fibre failure similar to that of the baseline specimens as described in Section 4.1. Immediately following fibre fracture in the central UD layers, the laminate as a whole delaminated from the shielding glass layers hence changing the colour visible to the naked eye of the observer – the orange colour on Figure 9 (a). A typical failure pattern of this configuration can be also seen in Figure 9 (a).

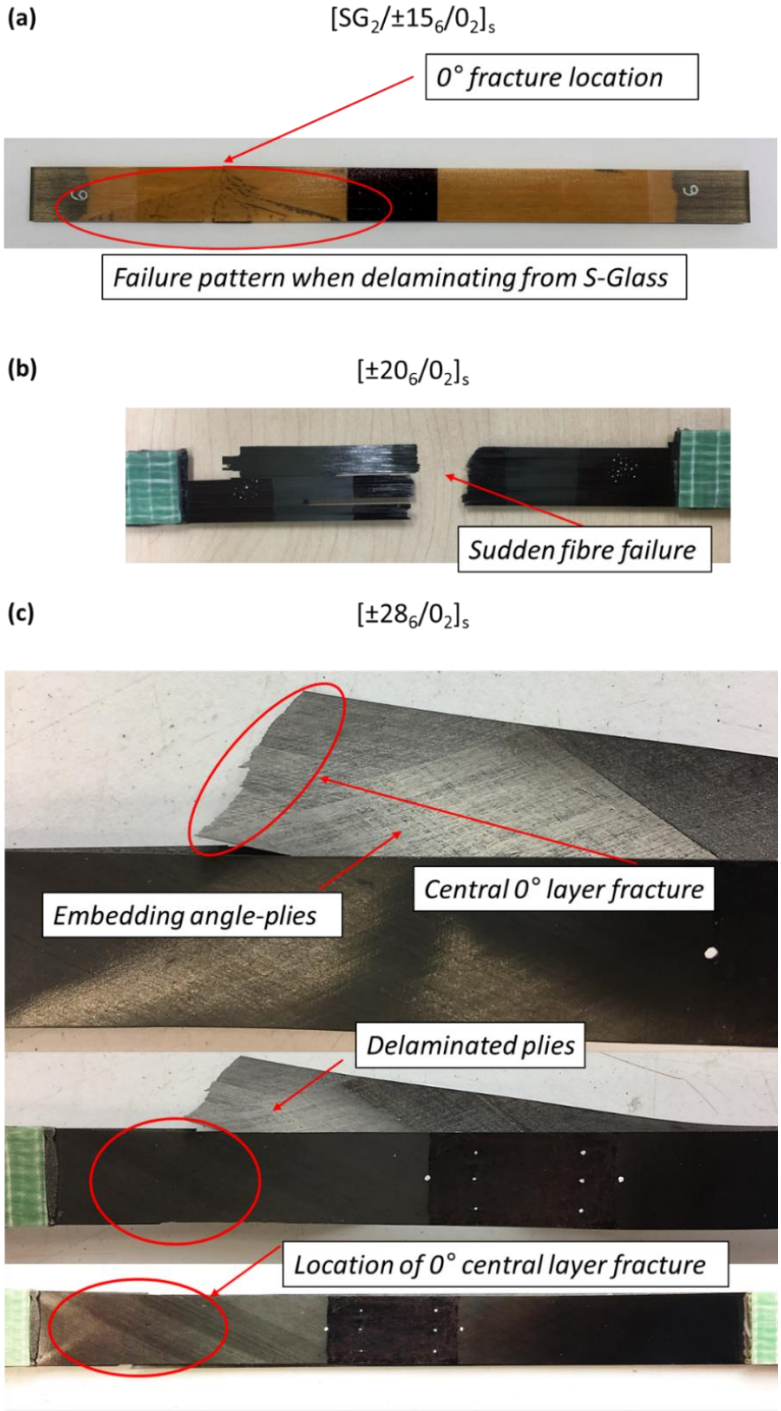

Figure 9. Illustration of the three configurations and their failure mechanisms: (a) $[SG_2/\pm15_6/0_2]_s$ hybrid configuration with 0° fibre fracture followed by delamination from the glass layers (b) $[\pm20_6/0_2]_s$ non-hybrid configuration with catastrophic 0° fibre failure and (c) $[\pm28_6/0_2]_s$ configuration with 0° fibre fracture followed by instant delamination from the angle plies

In contrast, the other two lay-ups of $[\pm 20_6/0_2]_s$ and $[\pm 28_6/0_2]_s$ were tested in a non-hybrid configuration, with end tabs. The $[\pm 20_6/0_2]_s$ type coupons exhibited a sudden fibre failure in the gauge section as it is shown in Figure 9 (b). This particular specimen also exhibits a secondary tab failure initiating from the end of the gauge section, but this did not cause the overall failure. The corresponding stress-strain curve in the mechanical test results (Figure 5 (c)) also exhibits a mostly linear behaviour up to failure. Both the 20- and 28-degree configurations exhibited similar strains to failure (1.62 % from Table 6) that correspond to the fibre fracture of the central 0° plies. An illustration of a failed 28 degree coupon is shown in Figure 9 (c). The central UD block that had delaminated from the surrounding angle-ply blocks was carefully pulled out in order to observe the fracture surface. The post-mortem examination of the specimens showed that the delamination initiated at the interface between the angle-ply and UD ply blocks at the location where the first fracture of the 0° layers occurred [41].

5. Conclusion

A novel design of composite tensile specimen was presented incorporating thin-ply, angle-ply/UD composites, where a multi-axial stress state of longitudinal tension and transverse compression is induced in the central 0° layers by the scissoring deformation of the embedding angle-ply blocks of the same material. The presented novel testing method is capable of generating reliable experimental data for a bi-axial stress state of longitudinal tension and transverse compression.

Three configurations were manufactured with variable amounts of transverse stresses generated in the central 0° layers. The 20° and 28° configurations exhibited an estimated maximum in-plane transverse compressive stress of about 140 MPa using linear calculations, although non-linearity would slightly reduce this value. When compared to the measured

baseline failure strain of the material, the significant transverse compressive strains applied – 2.84 % and 2.91 % for the 20° and 28° angle configurations respectively - did not significantly affect the overall strain to failure of the 0° plies.

Furthermore, the achieved in-plane compressive transverse strains are much higher than could be attained in a typical multi-directional laminate, exceeding the expected 90° fibre direction strain to failure. This suggests that in practice fibre direction tensile failure is not likely to be significantly affected by transverse compressive stresses. This result goes against interactive failure theories such as Tsai-Hill and Tsai-Wu which consider the interaction of longitudinal fibre tension and transverse compression to be important, but is consistent with the widely used maximum stress and strain criteria.

Acknowledgements

This work was partly supported by the Engineering and Physical Sciences Research Council through the EPSRC Centre for Doctoral Training in Advanced Composites for Innovation and Science (grant number EP/L016028/1). This work was also supported by the UK Engineering and Physical Sciences Research Council (EPSRC) Programme Grant EP/I02946X/1 on High Performance Ductile Composite Technology in collaboration with Imperial College London. Gergely Czél acknowledges the National Research, Development and Innovation Office (NRDI, Hungary) grant OTKA FK 131882 and he is also grateful for funding through the Premium Postdoctoral Fellowship Programme of the Hungarian Academy of Sciences. The data required to support the conclusions are provided within the paper.

References

[1] Wisnom MR. The Challenge of Predicting Failure in Composites. 19th Int Conf Compos Mater 2013:12–3. http://www.iccm-central.org/Proceedings/ICCM19proceedings/papers/WIS81754.pdf

[2] Quilter A. Composites in Aerospace Applications. Inf Handl Serv Inc 2004:1–5.

[3] Martínez-Barrera G, Gencel O, Reis JML. Civil Engineering Applications of Polymer Composites. Int J Polym Sci 2016;2016:1–2.

[4] Yangyang Q, Bisagni C, Bai Y. Experimental investigation and numerical simulation of unidirectional carbon fiber composite under multi-axial loadings. Compos Part B Eng 2017;124:190–206.

[5] Sun CT, Quinn BJ, Tao J. Comparative Evaluation of Failure Analysis Methods for Composite Laminates. U.S. Dep. Transp. Rep. no. DOT/FAA/AR-95/109, 1996.

[6] Tsai SW, Azzi VD. Anisotropic Strength of Composites derived from unidirectional specimens alone. Exp Mech 1965:283–8.

[7] Tsai SW, Wu EM. A General Theory of Strength for Anisotropic Materials. J Compos Mater 1971;5:58–80.

[8] Hinton MJ, Kaddour AS, Soden PD. Failure criteria in fibre reinforced polymer composites: the world-wide failure exercise. Elsevier; 2004.

[9] Kaddour AS, Hinton MJ. Maturity of 3D failure criteria for fibre-reinforced composites: Comparison between theories and experiments: Part B of WWFE-II. J Compos Mater 2013;47:925–66.

[10] Kaddour A, Hinton M, Smith P, Li S. A comparison between the predictive capability of matrix cracking, damage and failure criteria for fibre reinforced composite laminates: Part A of the third world-wide failure exercise. J Compos Mater 2013;47:2749–79.

[11] Hinton MJ, Soden PD, Kaddour AS. A Comparison of the Predictive Capabilities of

Current Failure Theories for Composite Laminates, judged against experimental evidence. Compos Sci Technol 2002;62:1725–97.

[12] Christensen RM. Why progress on the failure of fiber composite materials has been so retarded. J Reinf Plast Compos 2017;0:1–3.

[13] Welsh JS, Mayes JS. Recent biaxial test results of laminated composites and analytical MCT predictions. 49th Int SAMPE Symp Exhib Mater Process Technol - 60 Years SAMPE Progress, SAMPE 2004 2004:679–93.

[14] Chen AS, Matthews FL. A review of multiaxial/biaxial loading tests for composite materials. Composites 1993;24:395–406.

[15] Thom H. A review of the biaxial strength of fibre-reinforced plastics. Compos Part A Appl Sci Manuf 1998;29:869–86.

[16] Olsson R. A survey of test methods for multiaxial and out-of-plane strength of composite laminates. Compos Sci Technol 2011;71:773–83.

[17] Cohen D. Multi-Axial Composite Tube Test Method. Compos. Mater. Test. Des. Accept. Criteria, ASTM STP 1416, 2002.

[18] Swanson SR, Messick MJ, Tian Z. Failure of Carbon/Epoxy Lamina Under Combined Stress. J Compos Mater 1987;21:619–30.

[19] Welsh JS, Mayes JS, Biskner AC. 2-D biaxial testing and failure predictions of IM7/977-2 carbon/epoxy quasi-isotropic laminates. Compos Struct 2006;75:60–6.

[20] Welsh JS, Adams DF. An experimental investigation of the biaxial strength of IM6/3501-6 carbon/epoxy cross-ply laminates using cruciform specimens. Compos - Part A Appl Sci Manuf 2002;33:829–39.

[21] Pierron F, Vautrin A. The 10° off-axis tensile test: A critical approach. Compos Sci Technol 1996;56:483–8.

[22] Sun CT, Chung I. An oblique end-tab design for testing off-axis composite specimens.

Composites 1993;24:619–23.

[23] Jia H, Yang HI. Effect of shallow angles on compressive strength of biaxial and triaxial laminates. Springerplus 2016;5.

[24] Welsh JS, Adams DF. Testing of angle-ply laminates to obtain unidirectional composite compression strengths. Compos Part A Appl Sci Manuf 1997;28:387–96.

[25] Voloshin A, Arcan M. Failure of unidirectional fiber-reinforced materials—New methodology and results. Exp Mech 2006;20:280–4.

[26] Czél G, Jalalvand M, Wisnom MR. Hybrid specimens eliminating stress concentrations in tensile and compressive testing of unidirectional composites. Compos Part A Appl Sci Manuf 2016;91:436–47.

[27] Hart-Smith LJ. A Strain-Based Maximum-Shear-Stress Failure Criterion For Fibrous Composites. AIAA Struct. Struct. Dyn. Mater. Conf., Long Beach, California: 1990.

[28] Wisnom MR. The effect of transverse compressive stresses on tensile failure of glass fibre-epoxy. Compos Struct 1995;32:621–6.

[29] Swanson SR, Qian Y. Multiaxial characterization of T800/3900-2 carbon/epoxy composites. Compos Sci Technol 1992;43:197–203.

[30] Swanson SR. Strength design criteria for carbon/epoxy pressure vessels. J Spacecr Rockets 1990;27:522–6.

[31] Sun CT, Quinn BJ. Evaluation of failure criteria using off-axis laminate specimens. Am. Soc. Compos., 1994, p. 97–105.

[32] Catalanotti G, Camanho PP, Marques AT. Three-dimensional failure criteria for fiber-reinforced laminates. Compos Struct 2013;95:63–79.

[33] Wisnom MR, Czél G, Swolfs Y, Jalalvand M, Gorbatikh L, Verpoest I. Hybrid effects in thin ply carbon/glass unidirectional laminates: Accurate experimental determination and prediction. Compos Part A Appl Sci Manuf 2016;88:131–9.

[34] Sihn S, Kim RY, Kawabe K, Tsai SW. Experimental studies of thin-ply laminated composites. Compos Sci Technol 2007;67:996–1008.

[35] Xu X, Wisnom MR. An experimental and numerical investigation of the interaction between splits and edge delaminations in [+20m /-20m]ns carbon / epoxy laminates. Eur. Conf. Compos. Mater. - ECCM-15, 2012, p. 24–8.

[36] Fuller JD, Wisnom MR. Pseudo-ductility and damage suppression in thin ply CFRP angle-ply laminates. Compos Part A Appl Sci Manuf 2015;69:64–71.

[37] Cugnoni J, Amacher R, Kohler S, Brunner J, Kramer E, Dransfeld C, et al. Towards aerospace grade thin-ply composites: Effect of ply thickness, fibre, matrix and interlayer toughening on strength and damage tolerance. Compos Sci Technol 2018;168:467–77.

[38] Galos J. Thin-ply composite laminates: a review. Compos Struct 2020;236.

[39] Arteiro A, Furtado C, Catalanotti G, Linde P, Camanho PP. Thin-ply polymer composite materials: a review. Compos Part A Appl Sci Manuf 2020:105777.

[40] Laurin F, Carrère N, Maire JF. A multiscale progressive failure approach for composite laminates based on thermodynamical viscoelastic and damage models. Compos Part A Appl Sci Manuf 2007;38:198–209.

[41] Rev T, Czél G, Wisnom MR. A novel test method to induce bi-axial stress states in thin-ply carbon composites under combined longitudinal tension and transverse compression. ASC 33rd Annu. Tech. Conf. Compos. Mater., 2018.

[42] Fuller J. PhD Thesis - Pseudo-ductility of thin ply angle-ply laminates. University of Bristol, 2015.